https://doi.org/10.1038/s44453-026-00064-7

Exceptional observation of multiple electron radiation belts after the 11 May 2024 geomagnetic storm

Viviane Pierrard, Alexandre Winant, Edith Botek, Sylvie Benck & Stanislav Borisov

Check for updates

For the first time, four distinct electron belts were observed in the Earth's near-space environment after the exceptional geomagnetic storm of 11 May 2024. Usually, only two radiation belts are present: an inner and an outer belt, separated by a slot region. Although a three-belt configuration was previously reported once in 2012, our observations provide the first evidence that multiple-belt structures have occurred repeatedly following several geomagnetic storms since 2024.

The radiation belts were discovered by James Van Allen at the beginning of space exploration[1,2]. Under typical conditions, Earth's radiation environment consists of two belts: a stable inner belt filled by very energetic protons extending up to a few hundred Mega-electron Volt (MeV) and also by lower than a few MeV electrons trapped in the magnetic field of the Earth (e.g., refs. 3,4), and a much more variable outer belt, composed of relativistic electrons with energies above 500 keV that fluctuate with time scales ranging from minutes during geomagnetic storms to several days after the events (e.g., ref. 5). The two belts are separated by a relatively particle-depleted region known as the slot, located near 2.5 Earth radii (Re) in the equatorial plane. The flux variations are mainly due to solar wind fluctuations, as observed by multiple spacecraft (e.g., refs. 6,7). The high levels of radiation due to the very energetic particles of the Van Allen belts pose an important hazard to spacecraft and their crews.

The geomagnetic storm of 11 May 2024, also called the Mother's Day event, was the strongest storm in the last 20 years, with a Disturbance Storm Time index Dst = −412 nT[8]. It caused extraordinary modifications in the electron and proton radiation belts, observed by different spacecraft such as PROBA-V/EPT[8,9], METOP/MEPED[8], REPTile-2 on NASA's CIRBE[10], CSES[11], and NOAA satellites[12].

The present paper illustrates the four-belt structure of relativistic electrons that emerged after the storm, which had never been observed in the past. The additional belts resulted from localized electron depletion that created new slot regions, one very close to the inner belt and another in the middle of the outer belt. We show for the first time here that, although three belts had been observed only once previously, they have appeared repeatedly since 2024 following major geomagnetic storms in October 2024, June 2025, January 2026 and July 2026, coinciding with the recurrent formation of the deep inner slot.

Four belts after the 11 May 2024 storm

In the present work, we use the instrument EPT (Energetic Particle Telescope) developed by UCLouvain, BIRA-IASB and Redwire Space (previously called QinetiQ Space) and launched in May 2013 on board the ESA PROBA-V satellite in a Sun-synchronous polar Low Earth Orbit (LEO) at an altitude of 820 km[13,14]. The EPT detector measures electron differential flux from 0.5 to 8 MeV in 6 energy channels, and proton flux from 9.5 to 248 MeV in 10 energy channels. The EPT has been conceived to perform in-flight electron, proton, and heavy ion discrimination over a large energy range. The characteristics of the instrument and data were presented in detail in previous EPT articles[5,6,8,9,13,14] and are briefly remembered in the Supplementary file.

Here, we show in the schematic Fig. 1 the four electron belts observed during June 2024. The flux measured in the first channel of EPT for energies between 500 and 600 keV at an altitude of 820 km is mapped along the flux tubes of a dipolar magnetic field to provide a global representation of the toroidal structure of the radiation belts. The McIlwain parameter L corresponds to the distance in Re at which a magnetic field line crosses the geomagnetic equatorial plane. We define a belt as a local maximum in the flux and a slot as a local minimum in the flux, provided that the feature persists for more than 5 days (see profiles in Fig. S1). The four electron belts are well visible in Fig. 1 as yellow-orange toroidal regions separated by three darker slots. In general, only the darkest slot crossing the equatorial plane around 2.5 Re (1 Re = 6371 km) is present, separating the inner and outer

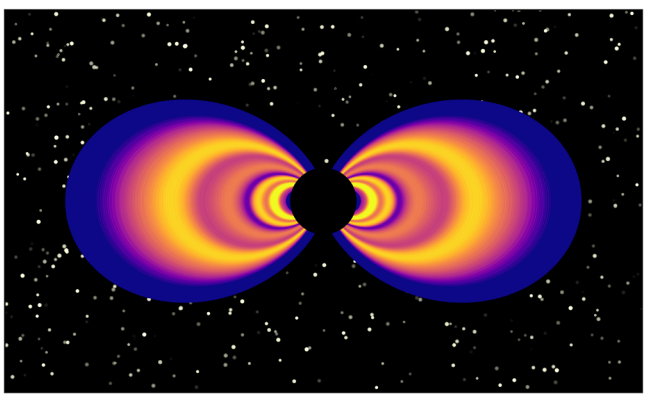


Fig. 1 | Four electron belts were observed in June 2024. This diagram is constructed by mapping the PROBA-V/EPT electron flux observed in June 2024 in channel 1 corresponding to 500–600 keV along dipolar magnetic field lines. The four belts correspond to the yellow-orange toroidal regions, while the three slots correspond to the darker purple areas separating them.

belts. The doughnut shape of the radiation belts is due to the motion of the particles along the magnetic field lines.

The four belts were also observed in higher-energy channels, the first five EPT channels between 500 keV and 2.4 MeV, as illustrated in Fig. 2 (and the profiles of Fig. S1), which also shows the formation and long-term evolution of the four belts. The fluxes are illustrated as a function of time and L, with fluxes averaged in L-shell bins of 0.1 L and temporal resolution of 1 day. The four-belt structure appears progressively several days after the extreme geomagnetic storm of 11 May 2024.

On 7 May 2024, before the storm, two belts are visible except in the last channel, 2.4–8.0 MeV, where no electrons are observed to be trapped in the inner belt at that time. In the first panel, for instance, the belts mainly correspond to the reddish regions. The inner belt located at L < 2.3 Re is very faint because there were no big storms previously. The outer belt is located at L > 2.8. They are separated by the slot (in green at that time in the first panel).

During the geomagnetic storm of 11 May 2024, the slot is filled, and one can also see later that the flux increases in the inner belt for all channels. Nevertheless, the lowest part of the slot remains visible, as the yellow horizontal line at L = 1.9 in the first panel, for instance. A few days later, the usual slot progressively reforms around L = 2.4, so that three belts are visible. It is only in June that another slot appears in the outer belt around L = 3.8, generating the four belts remaining visible for more than 4 weeks. At the end of June, a new storm intensifies the flux in the outer belt, filling it down to L = 3 and causing the extra slot in the outer belt to disappear. It slightly reappears a few days later[9] at a lower L (see light green in the first panel, for instance). The first slot of the inner belt at L = 1.9 gradually disappears, leaving a single inner belt. By August 2024, the two-belt structure had recovered, although the outer belt remained highly variable in response to geomagnetic activity. The 2.4–8 MeV channel shows only a faint split in the outer belt between the end of June and the beginning of August 2024. The belts are more visible in low-energy channels but are also well present in channel 5 (1–2.4 MeV), as illustrated in Figure S1.

Note that protons at E = 9.5–13 MeV were also exceptionally injected into the inner belt during this storm, as detected by PROBA-V/EPT and Reptile, for instance[8–10]. Protons have much longer lifetimes, so they are still present at the end of the year 2024, which enables us to discriminate well between the particles[9].

Repeated observations of three radiation belts between 2024 and 2026

An important discovery presented in this work is the presence of three belts several times between 2024 and 2026. Three electron belts were observed for the first time on 2 September 2012[15,16], three days after the launch of the twin Radiation Belt Storm Probes (RBSP) NASA spacecraft (decommissioned in 2019). The exceptional isolated third electron belt of E > 2 MeV due to a new slot in the outer belt around L = 3.8 persisted for four weeks. It was never observed again until the May 2024 event.

Figure 3 illustrates that three belts were again observed by PROBA-V/EPT in June and July 2025 for energies between 500 keV and 2.4 MeV, with distinct structures more visible for the lowest energy.

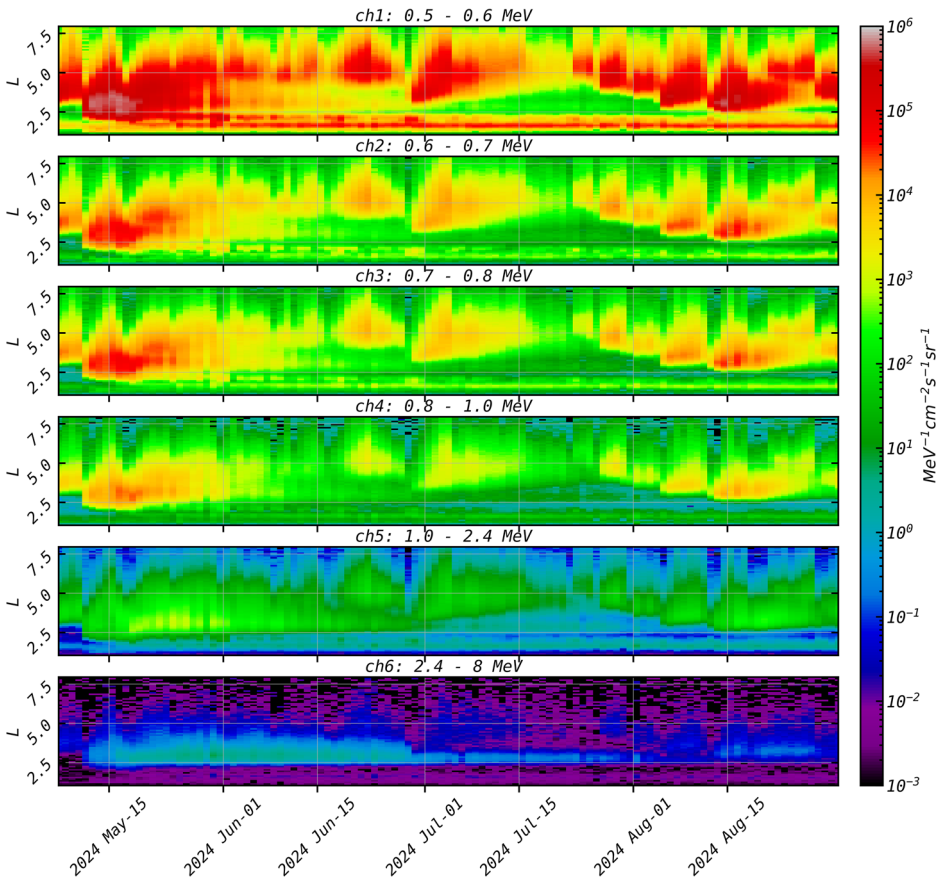


Fig. 2 | Differential electron fluxes measured from 7 May 2024 to 31 August 2024. Each panel corresponds to one of the 6 energy channels of PROBA-V/EPT, from 500 to 8 MeV. Four belts are observed in June 2024, except in ch6.

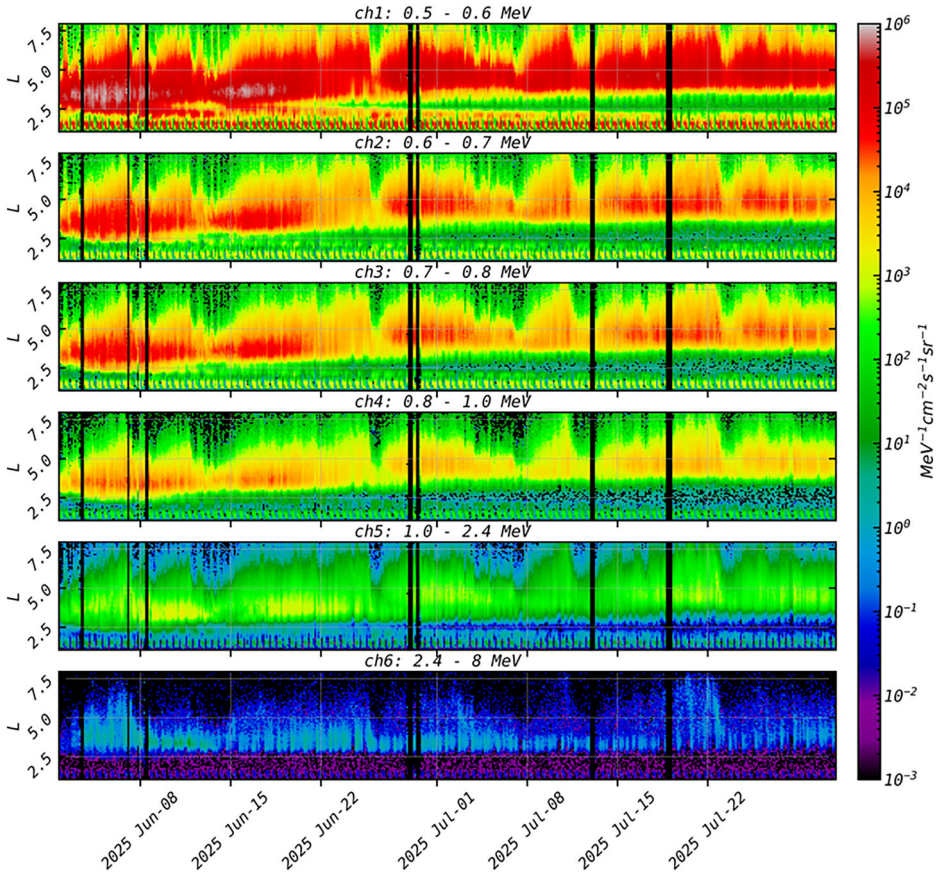


Fig. 3 | Differential electron fluxes measured from 1 June 2025 to 31 July 2025 in the 6 energy channels of PROBA-V/EPT. Three belts are visible from 10 June to mid-July 2025, except in ch6 above 2.4 MeV. The outer belt penetrates at lower L on 8 June 2025 due to geomagnetic activity, reducing the slot extension and its L position (see the yellow horizontal line around L = 2 in the top panel 1, for instance). Electrons are then trapped at L > 2, while the slot remains around L = 2. This is also well visible in other channels, although it becomes progressively less pronounced with increasing energy and is not observed in channel 6. A few days later, a new additional slot appears at L = 2.5. On 14 June 2025, a new injection fills the newly formed slot only in channel 1; however, the slot reforms on 18 June, resulting in a persistent three-belt configuration until the first slot gradually vanishes in July 2025, with the transition occurring earlier for higher energies.

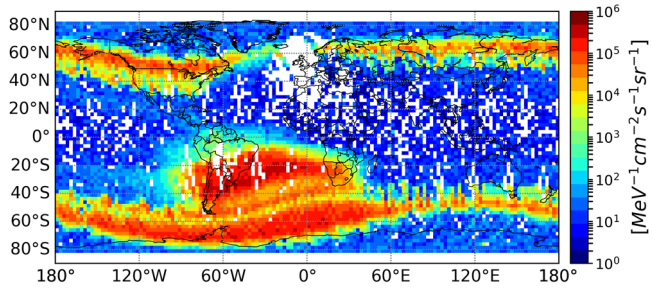


Fig. 4 | Three belts observed in the map of electron fluxes from 21 to 27 October 2024. The fluxes observed by PROBA-V/EPT at 0.5–0.6 MeV at the altitude of 820 km are averaged in bins of 2.5° in latitude and longitude.

Three belts are also observed by PROBA-V/EPT after other recent big geomagnetic storms: during one month after the 7–10 October 2024 geomagnetic storm (min Dst = −335 nT, the second strongest storm for the last 20 years[9]) (Fig. S2, top panel), in June 2025 (min Dst ~ −100 nT) (Fig. 3), in February 2026 (min Dst ~ −240 nT) (Fig. S3) and in July 2026 (min Dst ~ −150 nT) (Fig. S2 bottom panel).

The three-belt configuration forms through the same process that produced the first deep slot during the Mother's Day event: electrons are injected into the usual slot region, but penetrate only to a limited depth, depending on the intensity of the event and the electron energy range[17].

Three belts observed on maps at 820 km

The three belts are also visible in the maps of the electrons measured by PROBA-V/EPT at 820 km. Maps observed before and after the June 2025 event are illustrated in Fig. S4, with fluxes and pitch angles for this event also shown in Fig. S5. Figure 4 shows such a map for the October 2024 event, using channel 1 fluxes over 2.5° × 2.5° latitude–longitude bins between 21 and 27 October 2024. The high fluxes observed above South America and the South Atlantic correspond to the South Atlantic Anomaly associated with the inner belt[8,9]. This is due to the slight offset between the center of the Earth and the center of the geomagnetic field. The high-latitude bands correspond to the outer belt (e.g., ref. 18). The additional, unusual belt is visible between them (in red) in the Southern Hemisphere.

Causes of the new slots

Such three belts were not observed during storms of the previous solar maximum activity in 2014–2015[18]. The fluxes were directly injected into the inner belt, and the inner slot was not present (see Fig. S6). During the previous observation of three belts in 2012, the third belt resulted from the formation of a slot in the outer belt, similarly to the third slot observed in the May 2024 event.

The multiple Van Allen belts clearly appear due to the arrival of coronal mass ejections disturbing the space environment of the Earth and increasing the flux in the radiation belts. The storms with Dst < −100 nT inject electrons in the slot region with a depth that depends on Dst[17]. Some electrons are then trapped near L ~ 2, leaving a thin residual slot at L ~ 1.9 that

separates these newly trapped particles from those of the inner belt population. The presence of multiple belts depends on the energy. For October 2024 and July 2026, they are present mainly at 500–600 keV, while for the other events, they are also clearly visible for other energies below 1 MeV and even from 1 MeV to 2.4 MeV for May 2024.

Waves have been shown to play an important role in electron acceleration and loss in the radiation belts[19]. The formation of new slot(s) at high L-shells in the electron radiation belts is primarily due to the interaction of energetic electrons with VLF (Very Low Frequency) waves that scatter high energy electrons into the atmosphere. This can explain the new unusual slot caused a few days after the storm by the loss of electrons around L = 2–3, and at L ~ 3.5 in the case of the four belts. The main slot is associated with hiss resonance appearing inside the plasmasphere where background density is high[6,20]. Plasmaspheric hiss waves are modulated by variations in plasmaspheric density through local resonant amplification[21], which may explain why the slot can appear at slightly different L depending on the events. EMIC (ElectroMagnetic Ion Cyclotron) waves that are important at higher energy ($\gtrsim$1 MeV) and L > 1.5 have been shown to cause precipitation of radiation belt electrons (e.g., ref. 22). The multiple belt configuration typically persists for about one month, until the deep slot gradually disappears through radial diffusion[8].

The plasmapause gradient separates near-Earth space into zones of distinct dominant wave modes. Chorus waves generated beyond the cold background plasma of the plasmasphere contribute to the coupling between the plasmapause limit and the outer edge of the outer belt[23]. At L < 2.5, Coulomb scattering contributes significantly to radiation belt electron loss and is the dominant mechanism at L < 1.5[24].

The presence of the new multiple belts that were not observed during the previous solar cycle is due to the main slot penetrating at lower L than before (below L ~ 1.9). This is probably due to hiss wave activity that increases during geomagnetic disturbances in the slot region[25]. This may also be due to human activities' influence on the inner radiation belt. Indeed, high-power VLF transmitters used for submarine communication emit waves that scatter trapped electrons into the Earth's atmosphere[26]. These highly localized waves can produce the narrow slot at L < 2.5. Lightning-generated whistlers (300–30,000 Hz) within the plasmasphere can also cause electron losses at L < 3[27], but there is no evidence that their occurrence or intensity has increased in recent years. All these processes, i.e., hiss waves, lightning whistlers, VLF from transmitters, EMIC waves, Coulomb scattering, and chorus waves, contribute to energization, pitch angle scattering, and loss of radiation belt electrons, with complex interactions that can be better understood thanks to the most recent observations of high-resolution detectors. Understanding how these long-lived additional belts form and evolve provides new insight into the processes that trap and remove energetic particles in Earth's magnetic field. These processes will be investigated in more detail in future studies using simulations and models[28].

Data availability

The PROBA-V/EPT data are available in the public domain on the Space Situational Awareness website of ESA https://swe.ssa.esa.int/space-radiation. The data presented in this study are available at https://doi.org/10.18758/lu12i2kq.

Code availability

The codes generated during the current study are not publicly available due to privacy restrictions but are available from the corresponding author on reasonable request.

Viviane Pierrard[1,2] ✉, Alexandre Winant[1,2], Edith Botek[1], Sylvie Benck[2] & Stanislav Borisov[2]

[1]Royal Belgian Institute for Space Aeronomy, STCE and Space Physics, Brussels, Belgium. [2]Université Catholique de Louvain, Louvain-la-Neuve, Belgium. ✉e-mail: viviane.pierrard@aeronomie.be

Received: 30 July 2026; Accepted: 12 October 2026;
Published online: 16 November 2026

References

1. Van Allen, J. A. et al. Observation of high intensity radiation by Satellites 1958 Alpha and Gamma. *J. Jet Propuls* **28**, 588–592 https://doi.org/10.2514/8.7396 (1958).
2. Van Allen, J. A. & Frank, L. A. Radiation around the Earth to a radial distance of 107,400 km. *Nature* **183**, 430 https://doi.org/10.1038/183430a0 (1959).
3. Heynderickx, D. et al. A low altitude trapped proton model for solar minimum conditions based on SAMPEX/PET data. *IEEE Trans. Nuclear Sci.* **46**, 1475–1480 (1999).
4. Pierrard, V., Benck, S., Botek, E., Borisov, S. & Winant, A. Proton flux variations during solar energetic particle events, minimum and maximum solar activity and splitting of the proton belt in the South Atlantic Anomaly. *J. Geophys. Res. Space Phys.* **128**, e2022JA031202 https://doi.org/10.1029/2022JA031202 (2023).
5. Pierrard, V., Lopez Rosson, G. & Botek, E. Dynamics of megaelectron volt electrons observed in the inner belt by PROBA-V/EPT. *J. Geophys. Res. Space Phys* **124**, 1651–1659 https://doi.org/10.1029/2018JA026289 (2019).
6. Pierrard, V. et al. Observations and simulations of dropout events and flux enhancements in October 2013: comparing MEO equatorial with LEO polar orbit. *J. Geophys. Res. Space Phys.* **126**, e2020JA028850 https://doi.org/10.1029/2020JA028850 (2021).
7. Reeves, G. D. et al. Multi-platform observations of the radial penetration of substorm injected electrons and subsequent slot-filling event. *J. Geophys. Res. Space Phys.* **130**, e2025JA034329 https://doi.org/10.1029/2025JA034329 (2025).
8. Pierrard, V. et al. The Mother's Day solar storm of 11 May 2024 and its effect on Earth's radiation belts. *Universe 10* **10**, 1–18, https://doi.org/10.3390/universe10100391 (2024). 391.
9. Pierrard, V. & Winant, A. Atmospheric loss of energetic electrons and protons from the radiation belts after the exceptional injection of the 11 May 2024 superstorm leading to four electron belts. *Atmosphere* **17**, 1–24 https://doi.org/10.3390/atmos17030324 (2026).
10. Li, X. et al. A new electron and proton radiation belt identified by CIRBE/REPTile-2 measurements after the magnetic super storm of 10 May 2024. *J. Geophys. Res. Space Phys.* **130**, e2024JA033504 https://doi.org/10.1029/2024JA033504 (2025).
11. Zhang, Z. et al. The magnetosphere-ionosphere-ground responses to the May 2024 super solar storm. *Space Weather* **23**, e2024SW004197 (2025).
12. Xu, X. et al. Dynamics of proton flux in the south atlantic anomaly during the super geomagnetic Storm in May 2024. *J. Geophys. Res. Space Phys*. **130** https://doi.org/10.1029/2024JA033536 (2025).
13. Pierrard, V. et al. The energetic particle telescope: first results. *Space Sci. Rev.* **184**, 87–106 https://doi.org/10.1007/s11214-014-0097-8 (2014).
14. Cyamukungu, M. et al. The Energetic Particle Telescope (EPT) on board Proba-V: description of a new science-class instrument for particle detection in space. *IEEE Trans. Nuclear Sci.* **61**, 3667–3681 https://doi.org/10.1109/TNS.2014.2361955 (2014).
15. Baker, D. N. et al. A long-lived relativistic electron storage ring embedded in Earth's outer van allen belt. *Science* **340**, 186–190 https://doi.org/10.1126/science.1233518 (2013).
16. Shprits, Y. Y. et al. Unusual stable trapping of the ultrarelativistic electrons in the Van Allen radiation belts. *Nature Physics* **9**, 699–703 https://doi.org/10.1038/nphys2760 (2013).
17. Pierrard, V., Botek, E., Ripoll, J.-F. & Cunningham, G. S. Electron dropout events and flux enhancements associated with geomagnetic storms observed by PROBA-V/EPT from 2013 to 2019. *J. Geophys. Res. Space Phys.* **125**, e2020JA028487 https://doi.org/10.1029/2020JA028487 (2020).
18. Pierrard, V. & Lopez Rosson, G. The effects of the big storm events in the first half of 2015 on the radiation belts observed by EPT/PROBA-V. *Ann. Geophys.* **34**, 75–84 https://doi.org/10.5194/angeo-34-75-2016 (2016).
19. Horne, R. B. et al. Wave acceleration of electrons in the Van Allen radiation belts. *Nature* **437**, 227 https://doi.org/10.1038/nature03939 (2005).
20. Ripoll, J.-F. et al. Modeling of the cold electron plasma density for radiation belt physics. *Front. Astron. Space Sci* **10**, 1096595 https://doi.org/10.3389/fspas.2023.1096595 (2023).
21. Chen, L. et al. Modulation of plasmaspheric hiss intensity by thermal plasma density structure. *Geophys. Res. Lett.* **39**, L14103 https://doi.org/10.1029/2012GL052308 (2012).
22. Miyoshi, Y. et al. Precipitation of radiation belt electrons by EMIC waves, observed from ground and space. *Geophys. Res. Lett.* **35**, L23101 https://doi.org/10.1029/2008GL035727 (2008).
23. Pierrard, V. et al. Links of the plasmapause with other boundary layers of the magnetosphere: ionospheric convection, radiation belts boundaries, auroral oval. *Front. Astron. Space Sci.* **8**, 728531 https://doi.org/10.3389/fspas.2021.728531 (2021).
24. Claudepierre, S. G. et al. Empirically estimated electron lifetimes in the Earth's radiation belts: comparison with theory. *Geophys. Res. Lett.* **47**, e2019GL086056 (2020).
25. Meredith, N. P. et al. Origins of plasmaspheric hiss. *J. Geophys. Res.* **111**, A09217 https://doi.org/10.1029/2006JA011707 (2006).

26. Cunningham, G. S. et al. Observation of high-energy electrons precipitated by NWC transmitter from PROBA-V low-Earth orbit satellite. *Geophys. Res. Lett.* **47**, e2020GL089077 https://doi.org/10.1029/2020GL089077 (2020).
27. Feinland, M. et al. Lightning-induced relativistic electron precipitation from the inner radiation belt. *Nat. Commun.* **15**, 8721 (2025).
28. Ripoll, J.-F. et al. Particle dynamics in the Earth's radiation belts: review of current research and open questions. *J. Geophys. Res. Space Phys* **125**, e2019JA026735 https://doi.org/10.1029/2019JA026735 (2020).

Acknowledgements
All authors are grateful to the PROBA-V/EPT teams at B.USOC and ESA/Redu for their involvement in the data acquisition process. They also thank ESA/ESTEC for continuous support throughout the EPT mission.

Author contributions
Conceptualization, V.P.; Methodology, V.P. and A.W.; Software, A.W.; Validation, V.P., A.W., S.B., St.B.; Formal analysis, V.P. and A.W.; Investigation, V.P. and A.W.; Resources, V.P.; Data curation, A.W., S.B., St.B.; Writing—original draft preparation, V.P.; Writing—review and editing, V.P., A.W., E.B., S.B., St.B.; Visualization, A.W.; Supervision, V.P.; Project administration, V.P.; Funding acquisition, V.P. All authors have read and agreed to the present version of the manuscript.

Funding
This work is part of the RAISEARTH project that has received funding from the European Union's HORIZON INFRA program (Grant agreement GA 101289233). Funded by the European Union. Views and opinions expressed are however those of the author(s) only and do not necessarily reflect those of the European Union or the European Research Council Executive Agency. Neither the European Union nor the granting authority can be held responsible for them.

Competing interests
The authors declare no competing interests.

Additional information
Supplementary information The online version contains supplementary material available at https://doi.org/10.1038/s44453-026-00064-7.

Correspondence and requests for materials should be addressed to Viviane Pierrard.

Reprints and permissions information is available at http://www.nature.com/reprints

Publisher's note Springer Nature remains neutral with regard to jurisdictional claims in published maps and institutional affiliations.

Open Access This article is licensed under a Creative Commons Attribution-NonCommercial-NoDerivatives 4.0 International License, which permits any non-commercial use, sharing, distribution and reproduction in any medium or format, as long as you give appropriate credit to the original author(s) and the source, provide a link to the Creative Commons licence, and indicate if you modified the licensed material. You do not have permission under this licence to share adapted material derived from this article or parts of it. The images or other third party material in this article are included in the article's Creative Commons licence, unless indicated otherwise in a credit line to the material. If material is not included in the article's Creative Commons licence and your intended use is not permitted by statutory regulation or exceeds the permitted use, you will need to obtain permission directly from the copyright holder. To view a copy of this licence, visit http://creativecommons.org/licenses/by-nc-nd/4.0/.

© The Author(s) 2026